JOURNAL OF Materials Feature Article CHEMISTRY

Surface relief structures on azo polymer films

Nirmal K. Viswanathan,[ab] Dong Yu Kim,[bc] Shaoping Bian,[a] John Williams,[b] Wei Liu,[b] Lian Li,[d] Lynne Samuelson,[e] Jayant Kumar[ab] and Sukant K. Tripathy*[bc]

[a]*Department of Physics,* [b]*Center for Advanced Materials, and* [c]*Department of Chemistry, University of Massachusetts Lowell, Lowell, MA 01854, USA. E-mail: Sukant_Tripathy@uml.edu*
[d]*Molecular Technologies Inc., Westford, MA 01886, USA*
[e]*US Army Soldier & Biological Chemical Command, Soldier Systems Center, Natick, MA 01760, USA*

Received 26th March 1999, Accepted 17th May 1999

All optical fabrication of Surface Relief Grating (SRG) on azobenzene functionalized polymer films is reviewed in this article. The uniqueness of the single step erasable photofabrication of large amplitude surface relief structures on azo polymer films is mainly due to the photoisomerization and photoanisotropic behavior of the azobenzene group. The design and synthesis of several classes of suitable azobenzene functionalized polymers for the SRG formation is presented. Experimental studies are carried out in a systematic manner to understand the chemical and physical intricacies involved in the SRG formation process. Structural requirements and their limitations for the efficient fabrication of SRGs on azo functionalized polymer films are also discussed. Understanding the fundamental mechanism of SRG formation on the azo functionalized polymer films enables us to make use of these structures in a variety of applications.

Introduction

Azobenzene chromophore doped or covalently attached polymer systems, in the form of solid films, have been investigated for potential technological applications such as optical information storage and processing,[1–3] optical switching devices,[4,5] diffractive optical elements[6,7] among others. Some of the recent research interest in the azo dye containing polymer films includes fabricating integrated optical devices like channel waveguides,[8] polarization splitters,[9] nonlinear optical (NLO) devices[10,11] *etc.* Many of these applications are possible due to efficient photoisomerization and photoinduced anisotropy of the azobenzene groups. Historically, azo dye containing polymers were studied with immense interest for their unique photoinduced effects.[12–14] When illuminated with a polarized light of appropriate wavelength, the azobenzene groups undergo a reversible *trans*⇒*cis*⇒*trans* isomerization process and an associated orientational redistribution of the chromophores (Fig. 1). The versatility of these photoactive systems is that the azo groups can be selectively attached to the side chain, main chain or chain ends of a wide class of polymer systems. Appropriate substitution of the azobenzene chromophores may be used to tune the chromatic features from UV through the visible spectrum.[15] In addition, the possibility of achieving efficient optically induced effects even with low incident light power is advantageous.

In the initial years, kinetics of the photoinduced anisotropic effects were studied in solutions of azo dyes.[16,17] However, practical applications and device development required the use of solid films. Volume holographic gratings (or phase gratings) formed due to photoinduced alignment of the azo chromophores in thick azo dye doped polymer films have been studied for a long time.[18–24] Dramatic modification of the free surface

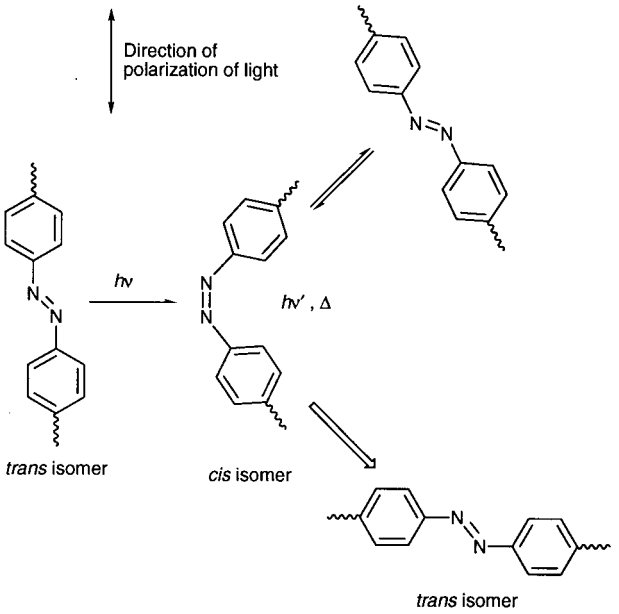

Fig. 1 Polarized light induced photoisomerization of azobenzene groups.

of a thin azo functionalized polymer film (thickness ≈1 μm), exposed to an interference pattern due to appropriately polarized light beams was only recently demonstrated[25,26] (Fig. 2). The sinusoidally modulated surface structures on the azobenzene functionalized polymer films, known as surface relief grating (SRG), are due to large-scale polymer chain migration. The formation of efficient SRG at a temperature substantially

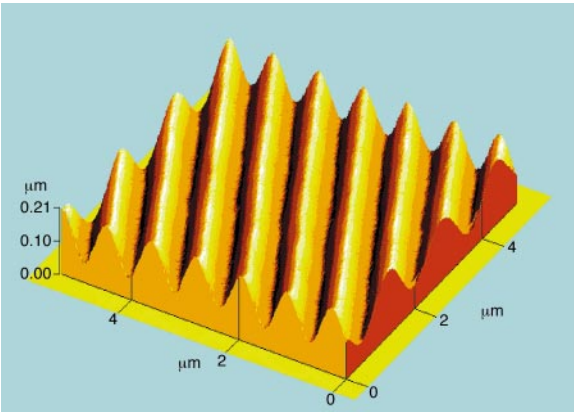

Fig. 2 Typical 3-D view of the SRG on the PDO3 film.

below the glass transition temperature (T_g) was not anticipated and presents new insight into photophysics of these polymer surfaces. The facile, all-optical, single step fabrication of high modulation depth SRGs in these polymers has presented a number of interesting possibilities since its discovery. Large amplitude SRGs in thin films of azo functionalized polymer with diverse chemical structures have been successfully written and the intriguing properties of the grating formation process continue to be reported.[27–30]

In this article, we review the extensive research that has already been reported by a number of groups on azo functionalized polymer materials for fabricating SRG. The photofabrication of surface relief structures on these polymer films is expected to have many interesting applications in photonics and the emerging area of nanotechnology. Our discussion begins by briefly mentioning the origin of the photoinduced anisotropy in azobenzene containing polymer systems. We then explain the experimental scheme utilized for photofabricating SRG on the azo polymer films. Azobenzene containing polymer systems are broadly classified as doped and functionalized systems. After a brief discussion on the azo dye doped polymer systems, we explain in detail the extensive and systematic research carried out by our group and others on the SRG formation in a variety of azobenzene functionalized amorphous polymer systems. In the process, we also mention the important chemical and structural requirements for the azo polymer materials in forming efficient SRGs. Research carried out on the liquid-crystalline (LC) azo polymer systems to form SRGs is briefly discussed in a subsection on functionalized azo polymers. Based on experimental observations on the important features, we have presented a mechanism for the SRG formation on azo functionalized glassy polymer films. Spatially varying optically induced anisotropy along with a component of electric field gradient in the direction of the grating vector are thought to be responsible for the large scale mass-transport of the azo functionalized polymer chains. Finally, the usefulness of the process is highlighted in the recent work on a variety of applications. We discuss some of the possible device applications based on the photofabricated diffractive optical elements, which are being explored in a number of laboratories.

Photoinduced effects in azo polymers

Azobenzene groups are known to exist in two isomeric states, a thermodynamically stable *trans* and a metastable *cis*. When irradiated with light of appropriate wavelength, the azobenzene chromophore undergoes a reversible *trans*⇒*cis*⇒*trans* photoisomerization process. Absorption of the appropriate wavelength light by the azo dye molecules elevates them to an electronically excited state. A non-radiative decay from the excited state puts the molecules back to the ground state either in the *cis* or the *trans* state. The metastable *cis* state goes to the *trans* state either by a spontaneous thermal back reaction or a reverse *cis*⇒*trans* photoisomerization cycle[13] (Fig. 1).

To begin with, the azo dye molecules are predominantly in the *trans* state at room temperature and are isotropically distributed. When excited by a linearly polarized blue-green light (488 nm), preferential molecular excitation and the associated photoisomerization process results in an orientational hole burning. The orientational redistribution of the dye molecules with respect to the polarization direction of the irradiating light finally leaves the *trans* isomers predominantly oriented perpendicular to this direction. Successive photoisomerization cycles result in a net dichroism and birefringence induced in the material due to the absorbance and refractive index difference in the parallel and perpendicular directions (to the incident polarization direction). The photoisomerization process, which implies mobility of the azo dye molecules, results in a facile change in its orientation due to the polarized optical field and has been observed even in high T_g polymer matrices.[31,32]

The polarized light induced anisotropy such as birefringence and dichroism in azo polymer materials is known to be due to the Weigert effect.[33,34] Optically induced orientation of an azobenzene chromophore (methyl orange) doped in a polymer matrix (polyvinyl alcohol) and related applications were first demonstrated by Todorov *et al.*[18–21] The photoinduced anisotropy and formation of birefringence gratings have since been studied in a variety of azo containing polymer systems including liquid crystalline[35–38] and amorphous polymers[39–43] as the matrix. Holographic gratings in photoanisotropic materials are recorded due to spatial variation of optical constants of the medium by superposing interferometrically produced spatially modulated light field patterns.[44,45] Azobenzene containing polymers, which belong to the class of photoanisotropic materials, respond to variations of both the intensity and polarization state of the total field.[23,24] Consequently, a pure spatially varying intensity distribution (scalar hologram), a pure spatially varying polarization pattern (polarization hologram) or a combination of both can be used to optically inscribe volume gratings. Researchers have modeled the scalar[46,47] and polarization volume hologram[20,22] to derive analytic formulae for the diffraction efficiency and to characterize the hologram. Polarization gratings were recorded with large diffraction efficiencies in the guest–host systems, utilizing the high sensitivity and large photoinduced birefringence of the azo polymer materials. However, the gratings do not have long term stability due to thermal randomization of the oriented azo dye molecules, even when stored in the dark. There has been concerted effort by several research groups to increase the stability of the photoinduced birefringence[31,32,48] and to understand and model the unique photoinduced anisotropic behavior of the azobenzene containing polymers.[49]

A large variety of azobenzene containing polymers with different chemical composition have been synthesized and used in the study of photofabrication of SRGs. In the following section, we discuss the details of the experimental setup used for fabricating surface relief gratings.

Photofabrication of surface relief grating

Surface relief grating can be photofabricated by a single step all optical process on azobenzene functionalized polymer films by superposing an interference pattern due to polarized light beams. A typical experimental setup used for the photofabrication of holographic SRGs is shown in Fig. 3 (the experimental setup used to fabricate SRG in the initial stages of research was slightly different[50,51]). An Ar^+ laser beam (typical wavelength for recording is 488 nm or 515 nm) is spatially filtered, collimated and then split by a beam splitter (BS) into two beams of equal intensity. The two beams after reflection from the mirrors (M_1 and M_2) are recombined to form an inter-

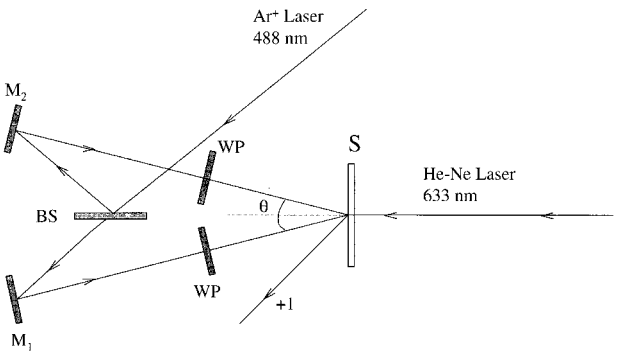

Fig. 3 Experimental setup for writing surface relief grating on azo functionalized polymer films. M_1, M_2: mirrors, BS: 50-50 beam splitter, WP: wave plate, S: azo polymer film, θ: interference angle.

ference pattern at the recording medium plane. The Ar^+ laser beam is linearly polarized in the vertical direction. The two interfering beams independently pass through half wave (or $\lambda/2$) plates to provide a control over the polarization state of the writing beams. Interfering beams with different polarization combinations were achieved by rotating the half wave plates. Replacing the half wave plates with quarter wave (or $\lambda/4$) plates, circularly polarized beams could be obtained.

Exposing the azo polymer film to the interference pattern due to appropriately polarized beams forms the SRG. The angle (θ) between the interfering beams can be adjusted to get desired periodicity (Λ) for the gratings. The results discussed in this article are for 1 μm period gratings, unless mentioned otherwise. The intensity of the writing beam monitored after the main beam is spatially filtered and collimated, ranges from 3 to 110 mW cm^{-2}. Typically, we use 50 mW cm^{-2} as the recording beam intensity in order to avoid any sample heating and spurious photothermal effects. The formation of SRG is monitored in real time by diffracting a low power (1 mW), unpolarized He-Ne laser (633 nm) from the spot where the two beams interfere. The +1 order diffracted beam from the grating in the transmission mode is detected and recorded. Fig. 4 shows a plot of the diffraction efficiency as a function of time. A 40 minutes exposure of the azo polymer film to the interference pattern created by two p-polarized laser beams can form a SRG with diffraction efficiency of 16% in each of the first order beams. After forming the SRG, the exposed region is scanned with an Atomic Force Microscope (AFM, Park Scientific, CA) in the contact mode. Fig. 2 shows an AFM image of a typical SRG formed on an epoxy-based azo polymer (PDO3) film. The SRG has a very regularly spaced sinusoidal structure with an amplitude modulation of 100 nm. The spacing is equal to the period of the interference pattern of 1 μm. The roughness of original film surface before exposure to the writing pattern is less than 0.5 nm.

The SRGs formed are stable when the polymers are kept below T_g. Heating the polymer films above T_g could erase the gratings in some cases. The gratings fabricated on a variety of azo functionalized glassy polymer films could also be erased by exposure to an appropriately polarized single laser beam.[52] During the SRG formation process, in addition to the photoinduced orientation of azo chromophores in these polymer films, there is large-scale macromolecular motion leading to the formation of the relief structure.

Azobenzene containing polymers

Azobenzene containing polymers on which photofabrication of SRGs has been attempted can be broadly classified into two groups: 1) azo dye doped polymers and 2) azo dye functionalized polymers. The azo chromophore functionalized polymer systems can be further divided into amorphous and liquid crystalline polymers. In the azo dye doped polymer system, also known as the guest–host system, the azo dye and the polymer are co-dissolved in appropriate solvents and coated onto glass slides to form films. In functionalized polymer systems, the azobenzene chromophore is covalently linked either as a side chain to the polymer backbone or in the main chain of the polymer. Liquid crystalline polymers with a pendant azobenzene group are due to linking of the different mesogenic groups to the polymer main chain through flexible alkyl spacers of varying lengths. Appropriately substituted azobenzene chromophores act as mesogenic units as well. In the following, we discuss the reported results of photofabrication of SRGs on each of the different classes of azobenzene containing polymers.

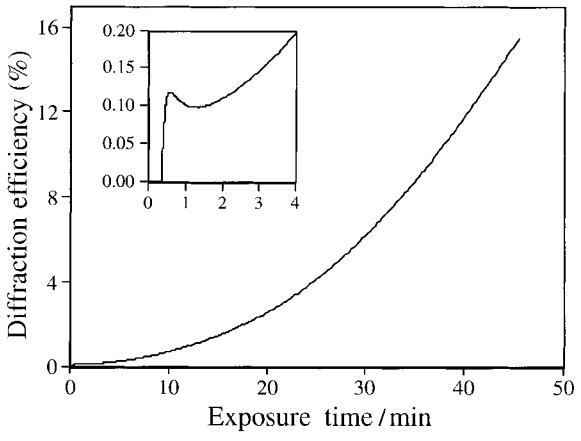

Fig. 4 Diffraction efficiency of the SRG photofabricated on PDO3 azo polymer film as a function of time. Inset shows initial stages of the grating formation.

Azo dye doped polymers. Samples of azo dye doped guest–host systems are made by dissolving azo dyes together with the host polymer in an appropriate solvent and films are formed from the solutions either by casting or by spin coating onto glass slides. The films are typically dried in a vacuum oven. The concentration of dye in the polymer is adjusted to produce homogeneous films. Film thicknesses typically range from a few millimetres to microns. Details of film preparation techniques of azo dye doped polymer films are discussed in the individual articles.

The discovery of SRG fabrication on the azo functionalized polymer films has renewed interest in the azo dye doped polymers.[27,53,54] Some of the recent research on the azo dye doped polymer systems is aimed at comparing the diffraction efficiency, birefringence and the formation of SRG with the functionalized systems to understand the fundamental process. In azo dye doped systems, the chromophores are not tethered to the polymer chains and their photoisomeric movements are not hindered by the polymer chains. Polymer chain migration, which is thought to be responsible for the large surface relief features, however, does not appear to occur. Consequently, the surface relief features are very weak as compared to functionalized polymers and the azo dye doped polymer films are not favorable for forming SRGs.

Azo functionalized amorphous polymers. Azobenzene functionalized amorphous polymer systems were the first to be investigated for SRG formation.[25,26] In the direct photofabrication of large amplitude holographic SRGs, the free surface of the azobenzene chromophore functionalized polymer thin film is dramatically modified when irradiated with polarized interfering light beam patterns.[25,26] A large variety of azo functionalized amorphous polymers with different chemical structures, molecular weights (MW) and glass transition temperatures (T_g) have since been extensively investigated.[27–29,50–52,55] Several of these investigations have been carried out to understand the effect of chemical and physical composition of the polymer systems in the formation of efficient SRGs. In the following subsections, approaches to the design and synthesis of several structurally diverse classes of amorphous azobenzene polymers and the SRG fabrication results are reviewed.

Side-chain azo polymer by direct polymerization. Chemical structures of a class of side chain glassy polymers on which the surface relief grating formation was first studied are shown in Fig. 5. The azo polymers were synthesized by addition polymerization of diglycidyl ether of bisphenol A with various primary amino functional azobenzene chromophores.[56] Good optical quality films were prepared by spin coating the azo polymer solutions on glass slides. Typical sample thicknesses of the films range from 0.4 to 1 μm and their T_gs range from 100 to 150 °C.

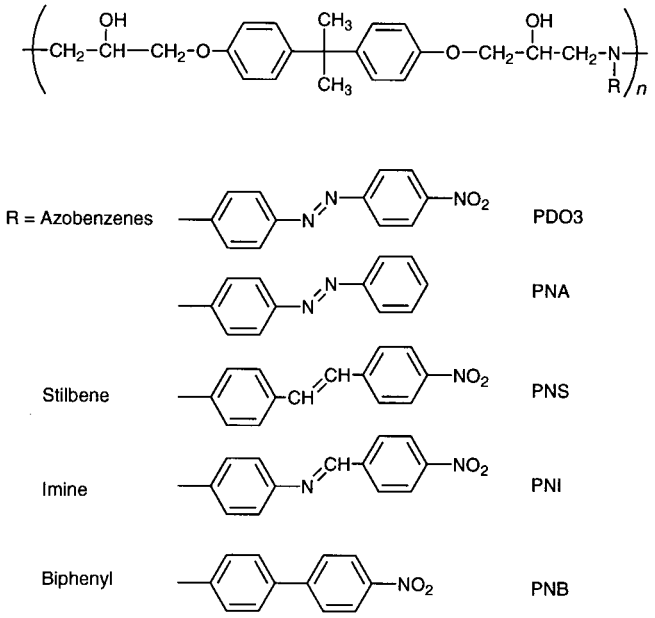

Fig. 5 Chemical structures of epoxy-based polymers synthesized by direct polymerization.

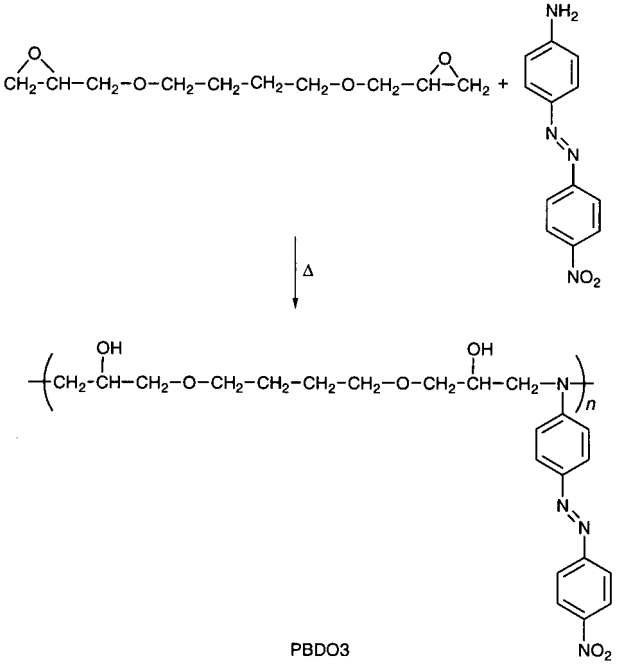

Fig. 6 Reaction scheme for the synthesis of low T_g azo functionalized PBDO3 polymer.

Fig. 4 shows a typical diffraction efficiency curve of the SRG formation process as a function of time. SRGs with large surface modulations could be formed on the polymers with azobenzene side groups, such as PDO3 and PNA. A typical three-dimensional view of the surface gratings on the polymer, PDO3, is shown in Fig. 2. As shown in the figure, the surface gratings showed a highly periodic sinusoidal pattern with a modulation depth of over 100 nm. The original film surfaces before exposure to the writing beams were planar, with less than a nanometer of rms surface roughness. The grating spacing was controlled by changing the angle (θ) between the two writing beams and was found to be consistent with the theoretically calculated spacing for the interference pattern. It is clear that the interfering polarized laser beams produced the surface relief patterns. Under the optimum conditions, surface modulation depth greater than 500 nm could be produced.

Among the side chain azo polymers listed in Fig. 5, PDO3 and PNA showed the formation of large amplitude SRGs. In case of the biphenyl side chain polymer, PNB, surface grating was barely observed under the same exposure level. Considering that the polymer PNB has the same backbone structure as PDO3 and PNA, it was inferred that the presence of azobenzene side groups which can undergo *trans*⇒*cis* photoisomerization is a critical structural requirement for the surface deformation process. To date this type of SRGs has only been found to form on azo functionalized polymer films. PNA was less efficient for surface grating formation than PDO3. It may be attributed to lower optical density of PNA at the writing wavelength. Furthermore, the acceptor substituted azo chromophore has higher polarizability, has shorter excited state lifetime[57] and hence cycles more often in the same time scale. It appears that strong electron donor–acceptor structure of the chromophore is helpful but is not a critical factor for the surface grating formation.

Polymers with stilbene (PNS) and imine chromophores (PNI) were also studied. These chromophores are known to be able to undergo *trans* ⇒*cis* photoisomerization process as well. However, the amplitude of surface grating produced was not appreciable in these polymer films. It is probably because both stilbene and imine groups require larger free volume ($\approx$224 Å^3) for the photoisomerization compared to the azobenzene groups (127 Å^3).[58] As a result, in this type of moderately high T_g polymer matrix, there may not be enough free volume for the photoisomerization of the stilbene and imine chromophores. In addition, the photoinduced orientation process of the chromophores was not observed with these polymer films either, as these groups are not expected to be as photoanisotropic as the azobenzene groups. Barrett *et al.* reported similar results from acrylate-based polymers (T_gs at around 100 °C) with DR1 type azo dyes in the side chain.[59] They also concluded that covalently attached azobenzene groups are necessary elements to observe the SRG formation process.

To study the effects of the mobility of polymer chains, an azo polymer with flexible alkyl chain backbone, namely, PBDO3, was synthesized (Fig. 6). The T_g of the polymer was about 35 °C as expected, given the flexible backbone. PBDO3, which contains the same azo chromophore but has a moderately rigid backbone, showed more than 20 times slower formation of the surface grating compared with PDO3. It appears that even if photoinduced surface deformation may be generated in this polymer, the deformation could not be fixed because of the fairly high mobility of the polymer molecules near T_g, resulting in relaxation to a smooth surface due to surface tension forces.

Side chain azo polymer by post-coupling reaction. Post polymerization azo coupling reaction can provide a convenient way to synthesize various azo functionalized polymers with different degrees of functionalization on the same backbone structure. It is often the simplest way to prepare azo functionalized polymers. In addition, versatile functional groups can be incorporated on the azobenzene moiety. Recently we have reported a series of polymers functionalized with azobenzene groups that were synthesized by post polymerization azo coupling reaction for the study of surface relief grating formation and NLO properties.[60,61] Polymers containing azo chromophores with ionizable groups could also be synthesized.[62] Under appropriate pH condition the polymers can be ionized into azo polyions in water. In a layer-by-layer electrostatic assembly process, along with an oppositely charged polyelectrolyte, the azobenzene polyelectrolyte can be assembled into multilayer films.[63] The chemical structures of the epoxy-based polymers post-functionalized with various azobenzene groups are shown in Fig. 7. The synthesis and

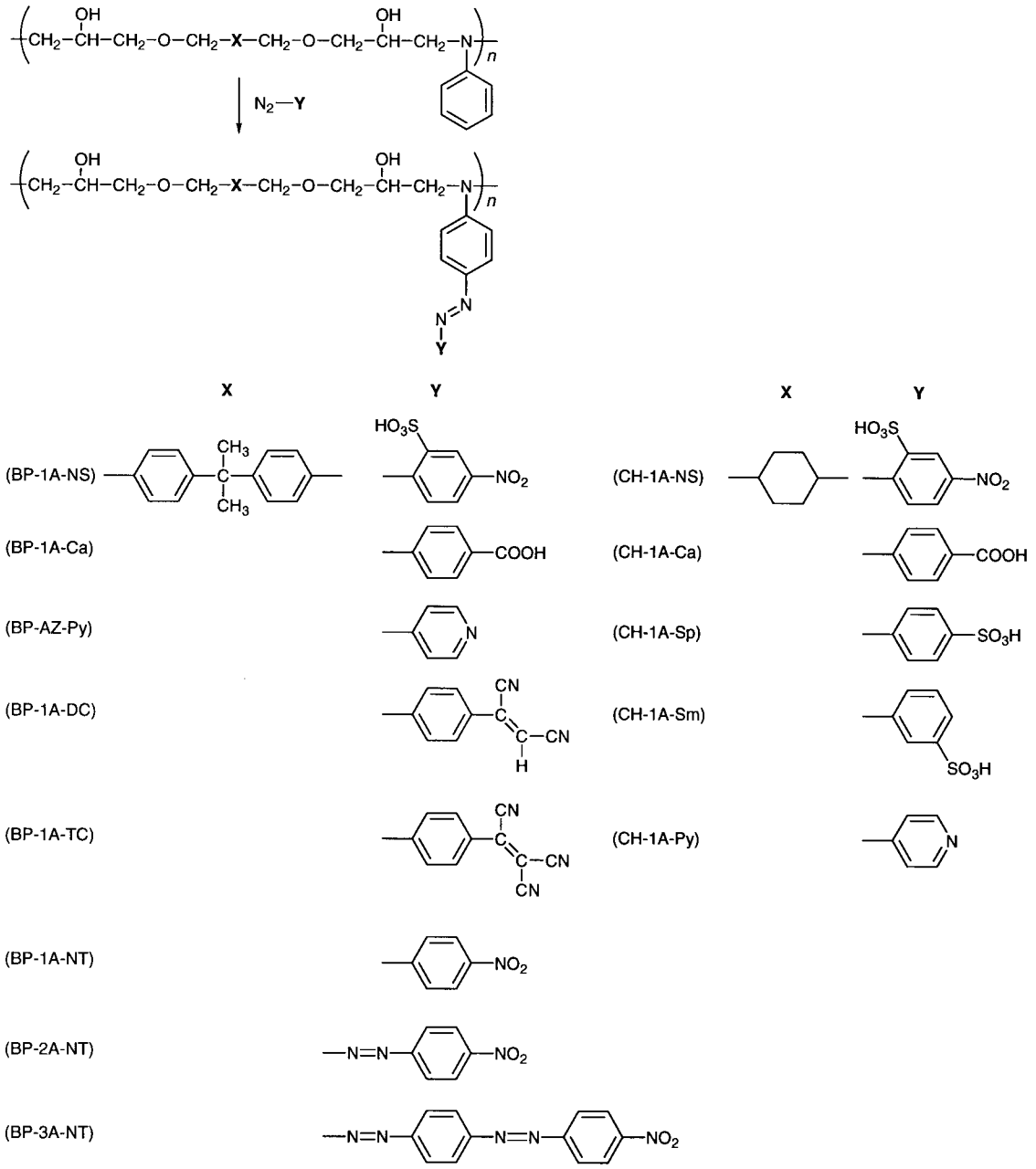

Fig. 7 Synthesis scheme and chemical structures of epoxy-based polymers post-functionalized with various azobenzene chromophores.

structure characterization of these epoxy based polymers have been reported elsewhere.[60–62]

Optical and thermal properties of some of these azobenzene polymers are listed in Table 1. The first part of the polymer nomenclature is an abbreviation to distinguish between precursor polymers from cyclohexane-1,4-dimethanol diglycidyl ether (CH) and the diglycidyl ether of bisphenol-A (BP). The subsequent parts refer to different conjugation bridges, electron acceptors and ionizable groups of the chromophores.

Table 1 Optical and thermal properties of the post azobenzene functionalized polymers

Polymer	D.F.[a] (%±3%)	λ_{max}[b]/nm (sol.)	λ_{max}/nm (film)	T_g/°C
CH-1A-NS	100	482	508	144
CH-1A-Ca	100	437	428	90
CH-1A-Sp	69	429	514	98
CH-1A-Sm	54	424	464	143
CH-1A-Py	100	440	437	88
BP-1A-NS	100	483		105
BP-1A-Ca	100	438		105

[a]Degree of functionalization measured by ^{1}H NMR. [b]In DMF solution.

The solubility characteristics of the synthesized polymers were greatly influenced by the chromophore and backbone structures. All of the polymers discussed above were able to form homogeneous solutions in polar organic solvents such as DMF. CH-AN based azo polymers containing acid groups such as CH-1A-NS and CH-1A-Ca are highly soluble in aqueous alkaline media. CH-1A-Py is soluble in aqueous acid solution. BP-AN based azo polymers containing acid groups such as BP-1A-NS are highly soluble in polar organic solvent, but can hardly be dissolved even in strongly alkaline aqueous solution. BP-1A-Py containing 4-(4-pyridylazo)aniline chromophores is not soluble in any solvent tested in our laboratory. The insolubility of BP-1A-Py is presumably due to the interaction between the pyridine nitrogen and the hydroxy groups on the main chain.

All the polymers exhibit thermal behavior typical of amorphous polymers. The T_g of the precursor polymer CH-AN is relatively low (41 °C) due to the flexible backbone. The

T_gs of the functionalized polymers are much higher than the precursor polymer and are highly dependent on the structure of the azo chromophores. CH-1A-CA and CH-1A-Py show T_gs of about 90 °C and the increase in T_g is attributed to a significant increase both in the size and the dipole moment of the side groups. CH-1A-NS and CH-1A-Sm show much higher T_gs (144 °C, 143 °C). It was shown from the UV–VIS spectroscopic studies that the polyelectrolytes containing sulfonic groups exhibit strong inter- and intramolecular interactions in the solid state probably resulting from the local charge separation.

It was found that these azo polymers show significantly different photoprocessability depending upon the chromophore structures. The polymers containing 4-(4-carboxyphenylazo)aniline chromophores such as CH-1A-CA and BP-1A-CA form surface relief gratings with large surface modulations and high diffraction efficiencies. As CH-1A-CA and BP-1A-CA possess polymer backbones with quite different rigidities, the similar recording efficiency for both polymers implies that the azo chromophores play the defining role in the grating formation process. Chromophore densities being similar, the two polymers are subjected to similar deforming forces and are equivalently photoisomerized in the writing process. The polymer containing 4-(2-sulfo-4-nitrophenylazo) aniline and 4-pyridylazoaniline chromophores such as CH-1A-NS and CH-1A-Py can form surface relief grating with low efficiency. In case of CH-1A-Sp and CH-1A-Sm, surface grating was hardly observed under the same recording conditions. It is believed that the driving force, resulting from localized variations of magnitude and polarization of the resultant electric field in the film, is counterbalanced by the strong intermolecular interaction mentioned above. Electric field induced poling experiments on these NLO polymers also indicated this strong intermolecular interaction to be present in sulfonic acid functionalized azo polymer systems. While the side chain azo polymers CH-1A-CA, BP-1A-CA and CH-1A-Py could be effectively poled, poling was inefficient for sulfonic acid functionalized azo polymer systems.

We have shown here that post-azo coupling is a convenient and versatile method for preparation of various kinds of azo polymers. One of the interesting properties of the azo polyelectrolytes such as CH-1A-CA is the unique ability to form both surface relief gratings and formation of multilayer structures by a layer-by-layer deposition process.

SRG efficiencies were also studied as a function of the molecular weight (MW) of the azo polymers. In high molecular weight azo functionalized acrylate systems, the gratings formed are similar to the ones formed in low MW (<5000 g mol^{-1}) systems but are less efficient. Synthetic details for preparing these very high molecular weight ($>500\,000$ g mol^{-1}) azobenzene functionalized copolymers are reported elsewhere.[63] The chemical structures of the two high molecular weight azobenzene functionalized polymers are shown in Fig. 8. The SRG formation behavior in the high molecular weight azo polymers is found to be less efficient, possibly due to expected chain entanglement. Barrett *et al.* further point out that in 50% blends of DR1 chromophore functionalized acrylic polymers (PDR1A) with PMMA of different molecular weights, surface deformation was still possible if the PMMA molecular weights were low and comparable to PDR1A. For much higher molecular weight PMMA, grating production was not possible and may be the result of excessive entanglement.[59]

SRG formation in side chain azo functionalized amorphous polymers with different chemical compositions have been reported by a number of laboratories.[28,29,64,65] Photoinduced translational diffusion of the azo chromophores in addition to their *trans–cis* isomerization cycles are judged to be responsible for the large amplitude holographic SRGs in the amorphous azo polymer films.[28] Photoinduced modification of the surface is also studied in polymer systems such as polyurethanes functionalized with azo dye,[29] and maleimide based high T_g amorphous terpolymers containing azo side groups functionalized to different degree.[65] In the polyurethane containing azobenzene system, apart from the mass transport of the polymer chains, some irreversible photochemical reactions have been suggested as the possible reason for the SRG formation.[29] SRGs fabricated on p(DR1M-*co*-MMA) by interfering two contrarotating circularly polarized light beams were used to study the orientational and angular distributions of the azobenzene chromophores by confocal Raman microspectrometry.[64] From the shapes of the distribution functions, photoinduced bulk transport effects are suggested to be responsible for the surface relief structures.

Main chain azo polymers. Most of the SRG formation experiments have been conducted on side chain azo functionalized polymer films. Main chain azo polymers, where the azobenzene groups are attached in the polymer backbones, have been investigated for the stability of photoinduced properties[12,14] and third order NLO properties.[66] In our laboratory, polyureas containing mono- and bisazoaromatic groups in the main chain were synthesized by condensation between isophorone diisocyanate and the corresponding diamines.[67,68] The chemical structures of PU1 and PU2 are shown in Fig. 9. Surface relief gratings could be fabricated on the films of these main chain azo polyureas with relatively high T_gs (PU1; 197 °C, PU2; 236 °C). The surface profile of the PU1 film (λ_{max} at 380 nm) after the formation of the gratings shows a

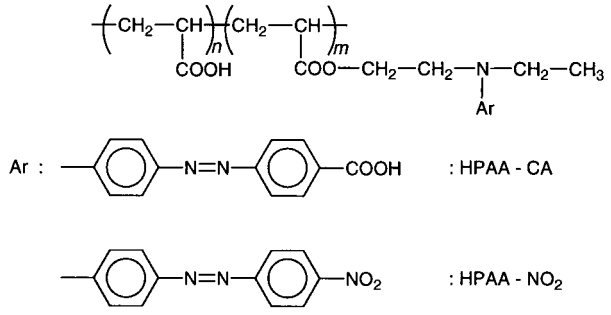

Fig. 8 Chemical structure of the high molecular weight side chain amorphous azobenzene functionalized poly(acrylic acid).

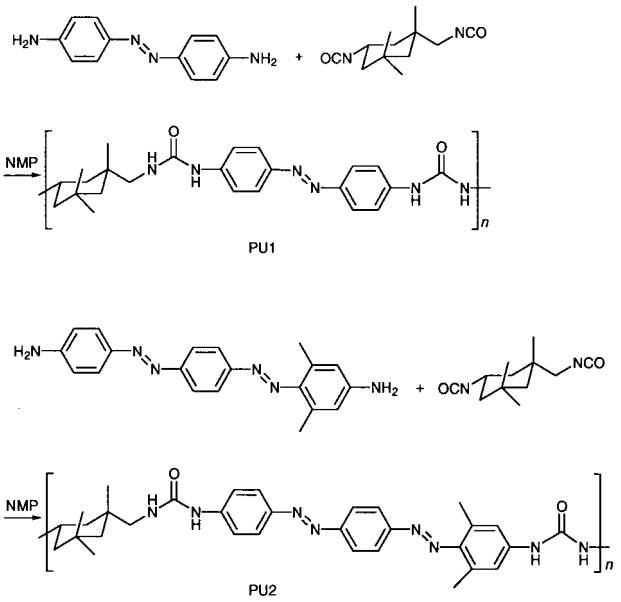

Fig. 9 Synthesis scheme and chemical structures of the main chain azo functionalized polyurea.

regular sinusoidal shape with a depth of about 44 nm and grating spacing of about 900 nm after exposure for 30 min. Under the same recording conditions, diffraction efficiencies and surface modulation were much larger in the side chain azo polymers. However, the modulation depths achieved are sufficient for fabrication of various types of diffractive optical components.

Grating formation on the film of polyurea with *bisazo*aromatic chromophores in its main chain (PU2) was also compared with PU1. The polymer film has λ_{max} at 393 nm and stronger absorption at 488 nm than the polyurea with *azo*aromatic chromophores (PU1). Regularly spaced sinusoidal surface relief gratings could be obtained on a film of PU2 as well in a manner similar to PU1. However, the modulation depth was even shallower and the diffraction efficiency was lower than that of PU1 for the same irradiation time. Photoinduced birefringence though small was also recorded for both PU1 and PU2.

As expected, the formation of the surface grating in the main chain polymers was much slower than the side chain polymers. This is because the polymer has a rigid backbone and the azobenzene groups are bound to the backbone at both ends, which restrict the mobility of the chromophores. However, when it is considered that these main chain polymers have very high T_gs, and relatively low absorption at the writing wavelength compared to the side chain polymers, the observation of the surface modulation is quite remarkable.

Conjugated azo polymers. Polymers with π-conjugated backbone electronic structures have been extensively studied for their unusual optical and electronic properties, showing most properties of their inorganic counterpart, the semiconductor materials. Recently, azo chromophores have been incorporated into the conjugated polymer structures such as polydiacetylenes[69] and polyacetylenes.[70]

A soluble polydiacetylene (PDA) functionalized with azobenzene groups in the side chain (Fig. 10) has been reported by Sukwattanisinitt *et al.*[69] Azobenzene functionalized PDA was prepared by post polymerization azo coupling reaction on the precursor PDA. The precursor PDA was reacted with the diazonium salt of *p*-aminobenzoic acid in *N*,*N*-dimethylformamide (DMF) to give a quantitative yield. The polymer was found to have 60% of the aromatic rings functionalized, by ^{1}H NMR. No T_g was observed from DSC studies of this polymer as it is expected to possess a rigid backbone with long persistence length. The surface grating formation in the PDA azo polymer system, post functionalized with azobenzene groups was investigated. Exposure of a spin-coated film to an interference pattern from two polarized argon-ion laser beams at 488 nm leads to the formation of a surface grating. The surface relief grating shows a very regularly spaced surface structure similar to other systems with depth modulation of over 80 nm. Even though the surface grating formation was less efficient than other epoxy side chain systems such as PDO3, and CH-1A-CA, it is very interesting to observe such a large and smooth surface modulation in a conjugated polymer system with a rigid polymer backbone. This result provided the first example of such laser-induced grating formation in a conjugated polymer lacking a glass transition. The surface grating formed on the conjugated polymers is expected to show interesting optical and electronic properties.

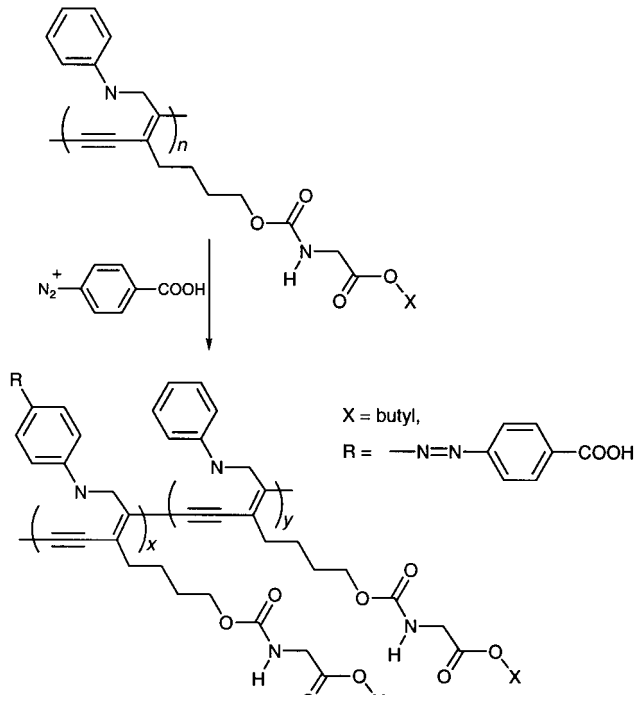

Fig. 10 Synthesis scheme of the polydiacetylene post-functionalized with azobenzene group.

Enzymatic synthesis of azo polymers. Enzyme catalyzed polymerization is a new methodology which is only recently been utilized to prepare diverse electroactive polymers.[71–73] This method also could be used to prepare conjugated aromatic macromolecular structures. We have synthesized novel photodynamic azo polymers such as poly(azophenol)[71,72] and polyaniline[73] containing azo chromophores by enzyme catalyzed polymerization. Phenols undergo polymerization, catalyzed by horseradish peroxidase (HRP), in the presence of hydrogen peroxide to yield an *ortho*-linked polymer with a polyphenylene backbone.[72] HRP catalyzed enzymatic polymerization of 4-phenylazophenol was expected to yield an azo polymer with the highest possible density of azobenzene chromophore in a polymer structure.

The final yield of the reaction carried out by enzymatic polymerization of 4-phenylazophenol at room temperature with HRP and H_2O_2 is 80%. GPC analysis estimates a molecular weight of the order of 3000 (MW) with a polydispersity of 3.5 and indicated a degree of polymerization of roughly 15. However, even this low degree of polymerization combined with excellent solubility is sufficient to produce optical quality thin films. Fig. 11(a) shows the reaction scheme and the chemical structure of this polymer and Fig. 11(b) shows the changes in the absorption spectra of poly(4-phenylazophenol) in dioxane after irradiation by 360 nm UV light. Interesting photoanisotropic properties of these polymer films have been investigated and high efficiency SRGs were fabricated in this class of macro dye systems. Synthesis, photoinduced optical properties and the SRG formation on this interesting new class of glassy 'macromolecular dye' are reported in detail elsewhere.[72]

Azo functionalized liquid crystalline polymers. Eich *et al.*[74,75] were the first to report optically induced birefringence and reversible optical storage on liquid crystalline (LC) azo polymer films. Since then there has been a lot of interest in the area of side chain and main chain liquid crystalline polymers with azobenzene group for optical data storage.[14,36] Optically stored information in the material is stable below the T_g of the liquid crystalline azo polymer and is expected to have long-term stability if the T_g is higher than the ambient temperature. However, similar to the amorphous azo polymers, the stored information can be erased by heating the material above its T_g. The main advantage of such a system is the high degree of field induced anisotropy achievable due to the mesogenic azobenzene group attached through flexible spacers. High storage densities, reversibility of information storage and short switching and access times are some of the important features making such systems widely researched.[14,36]

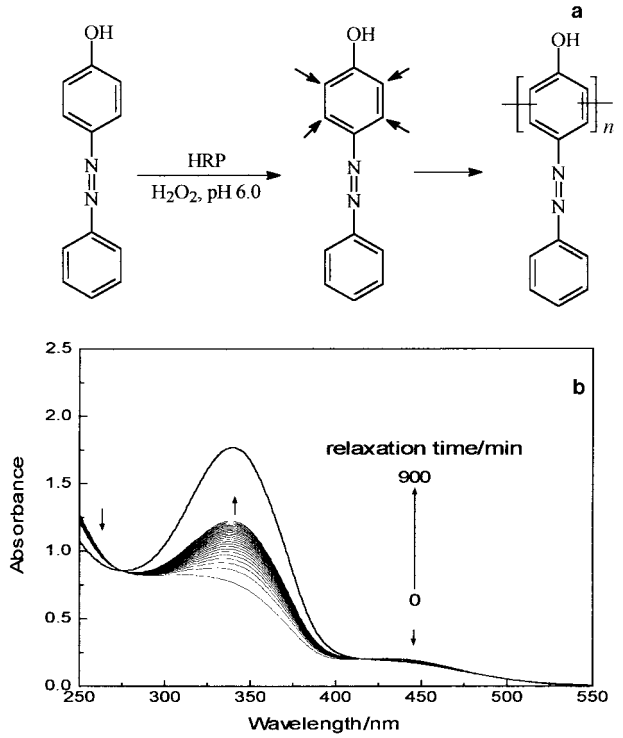

Fig. 11 (a) Reaction scheme for the enzymatic polymerization of poly(4-hydroxyazobenzene); (b) Absorption spectra showing the relaxation process of 4-phenylazophenol after photoexcitation at 360 nm.

Solid films of a variety of polyesters and polymethacrylates based liquid crystalline polymers are either solution cast or spin coated to typical thicknesses of 2–5 μm.[30,36,37,76,77] To begin with, the azobenzene side chain liquid crystal polymers were of interest only for long term storage of birefringence.[36,37,76,77] Optical storage properties,[78] linear and circular photoanisotropy[79] of the unoriented LC side chain azobenzene polymer films were studied by polarization holographic measurements. However, along with the birefringent grating, surface relief topographic gratings were recently observed in this class of polymers as well.[80,81] Typical intensities used to write the topographic gratings in the isotropic phase of the LC materials are high ($\geqslant 1$ W cm^{-2}). Polarization properties of diffraction at the gratings formed at low and high intensities are found to be different in the side chain azobenzene polyester films and under appropriate recording conditions result in the appearance of surface relief with doubled frequency.[82] The surface relief features are reported to be phase shifted as compared to that observed in amorphous azo functionalized polymer.[83] The difference in the behavior of the LC azo functionalized polymers as compared to the amorphous systems is explained on the basis of the attractive forces between the dipoles aligned parallel to the grating lines under suitable conditions.[84]

Mechanistic aspects of the SRG formation

The unique features observed during the all-optical fabrication of SRGs on azobenzene functionalized polymer films are summarized as follows: (1) large amplitude SRGs are formed only in the photoanisotropic azobenzene functionalized polymer thin films; (2) strong dependence on the polarization and on the energy (fluence) of the recording beams establishes this as a photonic process; (3) the SRGs are erasable both optically and thermally and after erasure they can be rewritten at the same spot many times without fatigue; (4) the large surface modulation of the SRGs is attributed to the macroscopic polymer chain migration assisted by the photoisomerizable azobenzene groups covalently attached to the polymer; (5) the mass transport of polymer chains by low power laser irradiation is most effective well below the glass transition temperature (T_g) of the polymer matrix; (6) the force responsible for the movement of the polymer chains is derived from the superposed optical field patterns; (7) the recording process is not a bulk process and needs an unconstrained surface. In the following, we discuss some of the experimental results and the different models proposed to explain the SRG recording process.

Polarization dependent writing process. The formation of SRG on azo polymer films is found to be strongly dependent on the polarization of the writing beams.[51,85] The diffraction efficiencies and the surface modulation of the SRGs recorded on the side chain azo functionalized CH-1A-CA polymer film under different polarization of writing beams are summarized in Table 2. Under the intensity recording condition, the two s-polarized writing beams produce the largest light intensity variation. However, there is no spatial variation in the direction of the resultant electric field and no component of resultant electric field along the grating vector direction. This configuration only produces a very low diffraction efficiency and small surface modulation for the SRG (<10 nm). Under the polarization recording conditions, the two writing beams have orthogonal polarization (s-p). The resultant electric field on the film surface has the largest variation but the light intensity is uniform over the entire irradiated area. Very small surface modulation and diffraction efficiency are obtained under this purely polarization recording condition. Under other recording conditions (p-p, $+45°$: $-45°$ and RCP: LCP), variations of both light intensity and the resultant electric field polarization on the film exist simultaneously.[85] The SRGs formed have much larger values for the surface modulation and diffraction efficiency. This indicates that the existence of both light intensity and resultant electric field variations are essential to the formation of SRGs on the azo functionalized polymer films. Several other researchers mentioned earlier report similar results on the azo functionalized polymers with different chemical compositions.

The SRGs formed on the azo functionalized polymer films are very stable at room temperature. Heating the sample above the glass transition temperature (T_g) can erase SRGs formed in most of the azo polymer systems. Recently we have also reported the unusual polarization dependent erasure behavior of the SRGs formed by exposure to a single laser beam of appropriate polarization.[52] This property has been utilized in fabricating phase masks and is discussed later.

Single beam experiment. To explore the grating formation mechanism and characterize the phase relationship between the relief grating and the interference pattern, a single Gaussian laser beam induced surface deformation experiment was carried out.[86] The experimental setup is schematically shown in Fig. 12(a). A He-Ne laser beam (544 nm), with a well-defined Gaussian light intensity profile is focused by a spherical lens.

Table 2 The diffraction efficiency (%) and surface modulation depth (nm) of the SRG fabricated on the CH-1A-CA azo functionalized polymer film under different recording conditions

Polarization of writing beams	Diffraction efficiency (%)	Modulation depth/nm
s:s	<0.1	<10
s:p	≈2	<20
p:p	5	50
$+45°$: $+45°$	0.1	<10
$+45°$: $-45°$	12.5	120
RCP:RCP	0.30	<10
RCP:LCP	22	250

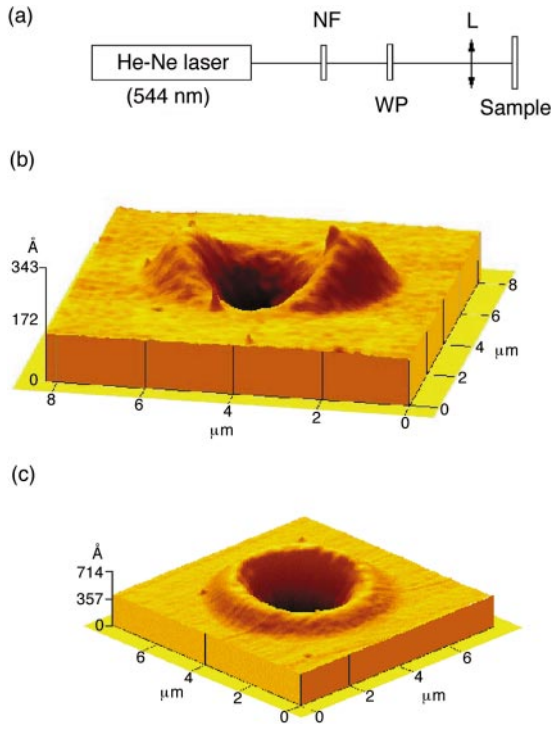

Fig. 12 (a) Single Gaussian beam experimental setup. NF: neutral density filter, WP: waveplate, and L: lens. AFM image of the surface deformation induced with (b) linear polarization and (c) circular polarization.

Different polarization states can be obtained by inserting a properly oriented waveplate. An epoxy-based azo functionalized polymer film (PDO3) is placed at the focal plane of the lens. The intensity of the laser beam is adjusted by inserting neutral density filters (NF). At the sample surface, the radius and central intensity of the laser beam are 3.0 μm and 328 mW cm^{-2}, respectively. The sample film is exposed for 70 min. Fig. 12(b) and 12(c) show a three-dimensional view of the surface exposed to linearly and circularly polarized Gaussian laser beams. The figures display two significant features. First, the photoinduced surface deformation exhibits strong polarization dependence. The maximum deformation occurs along the direction of laser polarization (assigned as the x direction in Fig. 12(b)). Second, the surface deformation profile along the polarization is not proportional (positively or negatively) to the laser intensity. Instead, it approximates to the second derivative of the laser intensity along the polarization direction (x-axis). These features further rule out the possibility of any thermal or laser ablative origin for the single laser beam induced surface deformation and the formation of topographic gratings.

Role of the free surface. It is well known that large values for birefringence in the azo polymer materials are due to the predominantly bulk nature of the photoinduced anisotropic variations of the azo chromophore. Contrary to some of the existing notions on the formation of SRG on azo polymer films as a bulk phenomenon,[59,84,87,88] we believe that the recording process needs an unrestricted surface. Details of the different approaches to understand the SRG formation process are discussed in the following section on mass transport process. The macroscopic movement of the polymer chains during the SRG formation begins at the free surface and continues through the bulk of the material as polymer layers are moved, to form large modulation depth gratings.

Experimental verification of the surface initiated SRG formation process is achieved by restricting the free surface of the azo polymer film in a precisely controlled manner.[63] For

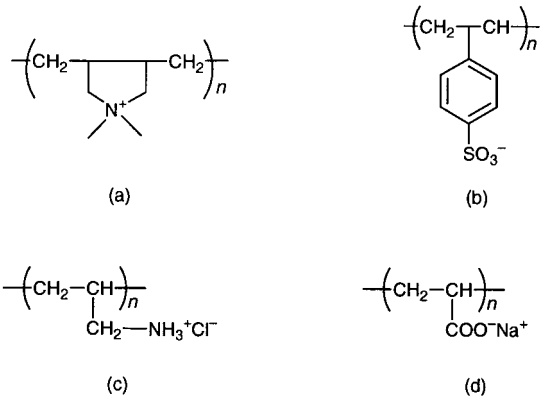

Fig. 13 Chemical structure of polyelectrolytes. (a) Poly(diallyldimethylammonium chloride): PDAC; (b) Sulfonated polystyrene: SPS; (c) Polyallylamine hydrochloride: PAH; (d) Poly acrylic acid: PAA.

this study, side chain azo functionalized polymers containing ionizable groups in the chromophores showing polyelectrolyte behavior under appropriate pH conditions were used. A recently reported technique of forming ultrathin polymer layers through an alternate layer-by-layer electrostatic deposition of oppositely charged polyelectrolytes[89] is made use of in our work. Chemical structures of the polyelectrolytes are given in Fig. 13. Constraining molecular layers are built in a well defined and controlled manner by depositing appropriate polyelectrolyte pairs on top of the spin coated azo polymer film substrates. This approach has the advantage of controlling layer thickness and organization at the molecular level.

The formation of SRG on the bare film and on the portions covered with ultrathin transparent polymer overlayers of different thickness is monitored by two different methods. Diffracting a He-Ne laser (633 nm) beam from the grating allows us to monitor the grating formation process as a function of time. A topographic scan of the irradiated region after the recording process, by an AFM, gives a measure of the modulation depth of the SRG formed. From these measurements, we can evaluate the importance of a free surface in the formation of SRG. The grating formation process in the region overlaid with ultrathin multilayer shows a drastically different behavior with increase in the number of bilayers. Both the SRG formation rate and the modulation depth of the gratings show an exponential decrease with increase in the number of bilayers (Fig. 14). In addition, the restraining influence of the ultrathin overlayers is found to be independent of the azo polymer and the polyelectrolyte pairs. Even a three-bilayer (4 nm maximum) overlayer on top of the azo polymer film is found to considerably slow down the grating formation process. Thicker ($\approx$25 nm) overlayers almost completely inhibit the surface initiated movement of the azo polymers while predominantly birefringent gratings without any surface features are easily formed.

Mass transport process. Several theories have been developed to understand the SRG formation process. Any proposed mechanism, in addition to explaining the many intricate aspects of this unusual mass transport process, must take into account the single most important feature, the strong polarization dependence of the recording process. Barrett *et al.*[59,87] have modeled the process based on pressure gradient induced deformation and the resulting viscoelastic flow to form surface gratings on the azo polymer films. The pressure gradients arise from the increased *cis* population in the bright regions, together with the *cis* isomer's large free volume requirement and the viscoelastic flow of the polymer is related to the velocity components by Navier–Stokes equations. Based on this, a relationship between the grating formation rate and intensity of the writing beams, molecular weight of the polymer and

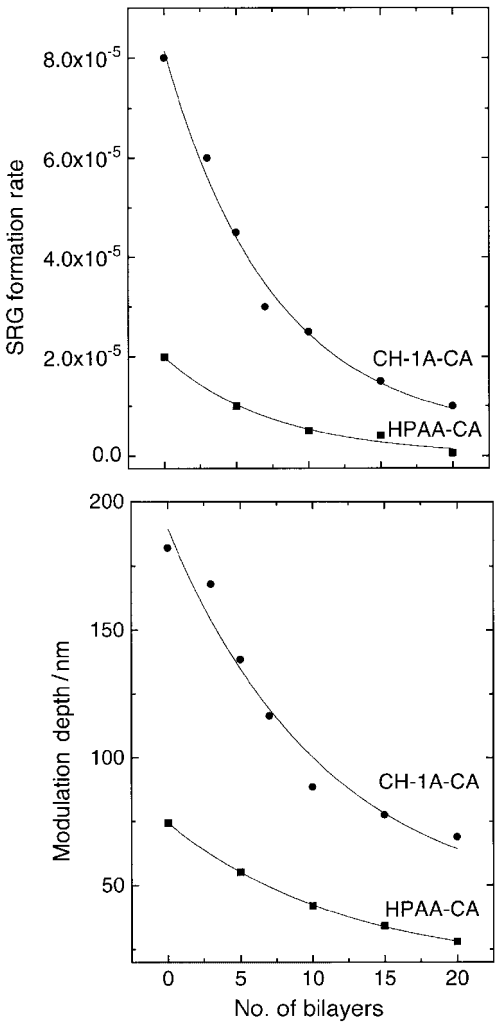

Fig. 14 Effect of the number of transparent polyelectrolyte bilayers on (a) rate of SRG formation, (b) modulation depth of the SRG.

thickness of the film is derived and experimentally verified. For thinner films, there is excellent agreement of the experimentally observed and predicted writing efficiency and film thickness. Inscription rate is found to increase linearly as a function of light intensity and is accurately accounted for by this model. The gradient of isomerization pressure model however, does not adequately account for the strong polarization dependent grating formation process.

A mean-field model was proposed by Pedersen *et al.*[84] to explain the SRG formation in side chain LC azo polymers. According to this model, the photoinduced alignment of chromophores in the illuminated regions, together with an attractive force when the chromophores lie side-by-side, induces polymer flow towards the bright regions. Theoretical predictions of the polarization dependence of the periodicity and shape of the surface relief profiles have been found to agree well with the experimental results. However, the model presumes a spatially constant intensity when two orthogonally polarized beams interfere at an angle ($\theta > 0$). This treatment, based on the intrinsic mobility of the LC materials, does not account for the dip (instead of peak) inscribed in the material where the intensity is maximum, observed in the amorphous azo polymers.[82,83]

Lefin *et al.*[28,88] have proposed an anisotropic diffusion mechanism incorporating the optical polarization direction into a photoinduced pressure model. According to this model, as the optical field excites the azo chromophores aligned parallel to the polarization direction, the photoisomerization cycle translates the azo functionalized polymer along their long axis in an '*inchworm*' like fashion. The resulting translationally activated population would then diffuse from the bright regions outward along the polarization direction. This model does not consider the well-known photoinduced reorientation of the azo chromophore during the course of SRG formation. In addition, there is no known mechanism whereby the anisotropic diffusion could be coupled to the polymer chain migration without scattering or randomization.

Our approach to understanding this problem has focused on forces derived from optically induced electric field gradient.[90] Interaction of the azo chromophore functionalized macromolecules with the optical field induces polarization in the material in the direction of the field. Efficient *trans*⇒*cis*⇒*trans* photoisomerization cycling leads to a photostationary state when there is a net chromophore orientation perpendicular to the field direction. The associated decrease in the refractive index and hence the susceptibility of the material defines the direction of flow[91] of the polymer chains. The unique aspect of the azo polymer system is that these processes occur simultaneously and the time averaged effect results in transport of the polymer chains in the field gradient direction. The process is initiated at the film surface and continues through the bulk of the material as the polymer layers are moved, leading to high amplitude gratings. The force responsible for the movement of the polymer involves a spatial variation of the susceptibility of the material and an electric field gradient.

In a polarizable polymer medium, the time averaged optically induced gradient force density f is given by eqn. (1)

$$\vec{f} = \langle [\vec{P}(\vec{r},t)\bullet\vec{\nabla}]\vec{E}(\vec{r},t)\rangle$$
$$\text{with } \vec{P}(\vec{r},t) = \varepsilon_0\chi\vec{E}(\vec{r},t) \qquad (1)$$

where $< >$ is for the time averaged process and $E(r,t)$, $P(r,t)$, ε_0 and χ represent the optical field, the optically induced polarization, the permittivity of free space and the susceptibility of the medium respectively. Eqn. (1) implies that the polymer chains experience a force only when there is a component of optical field gradient along the polarization direction. For a cylindrical Gaussian beam, whose optical field amplitude is described by $E(x) = E(0)\exp(-x^2/\omega^2)$ the force density, according to eqn. (1) is described by eqn. (2)

$$f(x) \propto \chi' \mathrm{d}I(x)/\mathrm{d}x \qquad (2)$$

where $I(x)$ is the intensity distribution of the Gaussian beam and χ' is the real part of the susceptibility. The single beam experimental results reveal that the polymer chains move out from the light irradiated region to the non-irradiated region. The force direction is away from the center of the beam implying that $\chi' < 0$.[91] In the grating experiment, the driving force responsible for the macroscopic movement of the polymer chains at the free surface of the polymer film can be written as[85] in eqn. (3)

$$f_x = \varepsilon_0\left[\chi'_{ix}E_x\frac{\partial}{\partial x}E_x\right] \qquad (3)$$

where the subscript '*i*' stands for the spatial coordinates x, y, z. The change in the susceptibility of the medium, $\chi' = \chi \pm \Delta\chi$ includes the susceptibility of the medium (χ) before irradiation and spatial variation of the optically induced change $\Delta\chi$. Thus, the spatial variation of susceptibility (χ') along with a component of the field gradient in a direction parallel to the grating vector (x-axis) are the factors responsible for the SRG formation on azo functionalized polymer films. The time averaged nonzero force due to the above-mentioned factors acting on the azobenzene chromophore tethered polymer chains results in the macroscopic movement of the polymer chains and hence the formation of SRG. This mechanism explains the surface initiated and strong polarization dependent recording process for SRG formation on the azo functionalized amorphous

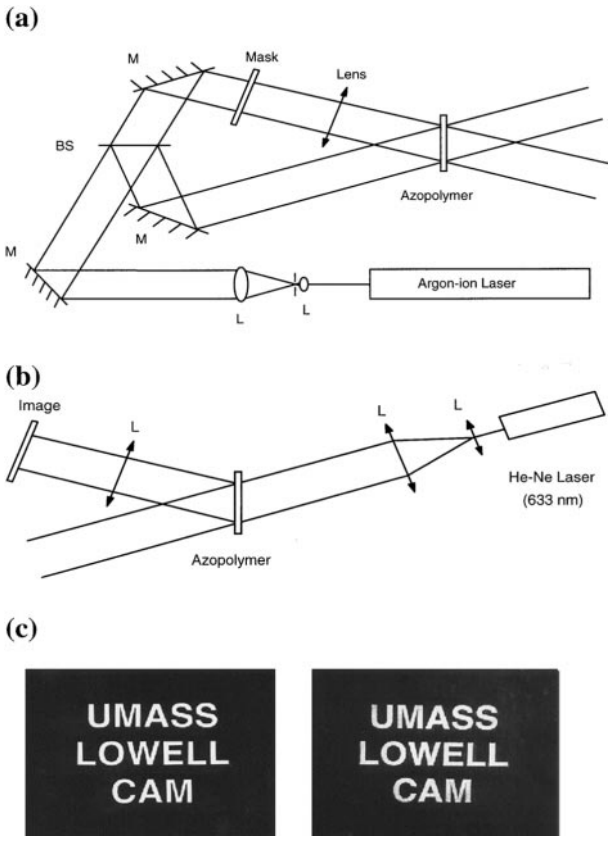

Fig. 15 (a) Holographic recording setup, (b) reconstruction setup. L: lens, M: mirror, BS: beam splitter, (c) photograph of the mask (on the left) and replica (on the right).

polymer systems. The model has also adequately accounted for the observed surface relief features in this class of azobenzene functionalized polymer films. We discuss in the following section some interesting and diverse applications utilizing the unique photoinduced optical properties of the azo polymer films.

Applications

1(a). Holographic image storage and retrieval. Fig. 15 gives a schematic of the experimental setup for holographic image storage and retrieval in an azo functionalized polymer film. A laser beam ($\lambda = 488$ nm) from an argon-ion laser is expanded and collimated by a lens system and then is split by a beam splitter (BS) into two beams. An object mask is placed in the path of one of the beams. The beam carrying the object mask information interferes with another collimated beam at the recording medium plane. Exposing the interference pattern onto the azo polymer film formed a surface relief hologram. The retrieval of the stored information is accomplished by a holographic reconstruction setup shown in Fig. 15(b). A He-Ne laser ($\lambda = 633$ nm) was expanded and used to reconstruct the holographic image. Fig. 15(c) shows the object mask on the left and the reconstructed image on the right.

1(b). Mask and copy. Phase masks[92,93] have been extensively utilized to produce periodic light intensity modulation. They have been employed to fabricate not only fiber gratings but also thin-film gratings[94] and surface relief gratings on glass.[95] Recently, Jiang *et al.*[52] have successfully demonstrated that the surface relief gratings written on the azobenzene functionalized polymer films can be used as phase masks. Application of the surface relief gratings as phase masks written with appropriate polarization on the azobenzene polymer films, to replicate the grating structure on other azo

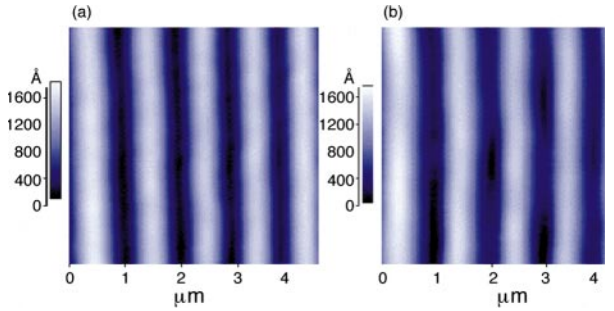

Fig. 16 AFM images of (a) mask and (b) replica grating.

functionalized polymer films, has been accomplished.[52,96] A phase mask of 900 nm spacing was fabricated by interfering two 488 nm Ar^+ laser beams on an azo polymer film (PDO3). The polarization of the writing beam is set at an angle of 45° with respect to the *s*-polarization. The mask was then replicated onto another film of similar azo polymer by photoprinting, using a single beam exposure at 514 nm with a polarization perpendicular to the grooves of the mask. Under this polarization condition, no erasure of the mask during the photoprinting process was observed.[52] Fig. 16 shows the AFM images of the phase mask and the replica grating produced from the mask. The period of the replica grating is identical to that of the phase mask, which has resulted from an interference of the zeroth and the first order diffracted beams. The desired modulation depth can be achieved by controlling the exposure conditions.

2. Polarization discriminator. A strong dependence of diffraction efficiency on the state of polarization of the probe light is well known in volume holograms.[24,97] Investigation of the polarization properties of the SRGs formed due to the photoanisotropic interaction leads to several interesting results. Our recent studies on the polarization diffraction properties of the SRGs formed on azo functionalized polymer films show a strong dependence on the polarization state of the probe beam. The dependence on the diffraction efficiency of the probe beam polarization can be used as a polarization discriminator.

To achieve high polarization discrimination capabilities, the gratings should have special surface relief profiles with periodicity (Λ) comparable to the wavelength of the probe light beam (λ_p).[98] However, these are difficult to achieve under normal laboratory conditions. Here we have demonstrated that SRGs written on the azo polymer films have the advantage that even when $\Lambda > \lambda_p$, it is possible to achieve the desired polarization selective optical function. This unique feature is thought to be due to the simultaneous inscription of both anisotropic and surface relief gratings on the azobenzene functionalized polymer films.

In our experimental investigation, SRGs were initially fabricated using interference of two opposite circularly polarized Ar^+ laser beams. This configuration is known to introduce a large anisotropy and fabricate large amplitude relief gratings on the azo polymer (CH-1A-CA) films. The gratings are of 1 μm period with modulation depth of 150 nm. The +1 order diffracted beam of an unpolarized He-Ne probe beam (633 nm) at normal incidence after passing through the grating is analyzed and found to be predominantly horizontally polarized. Schematic of the polarization discriminator function of the SRG is shown in Fig. 17(a). The polarization discriminating capability of this grating between the vertical and horizontal components of the probe is 1 part in 8 and is shown in Fig. 17(b). Further research is in progress to increase the polarization discriminating capabilities of the SRGs formed on azo polymer films. We feel that stacking the gratings together could increase this effect.

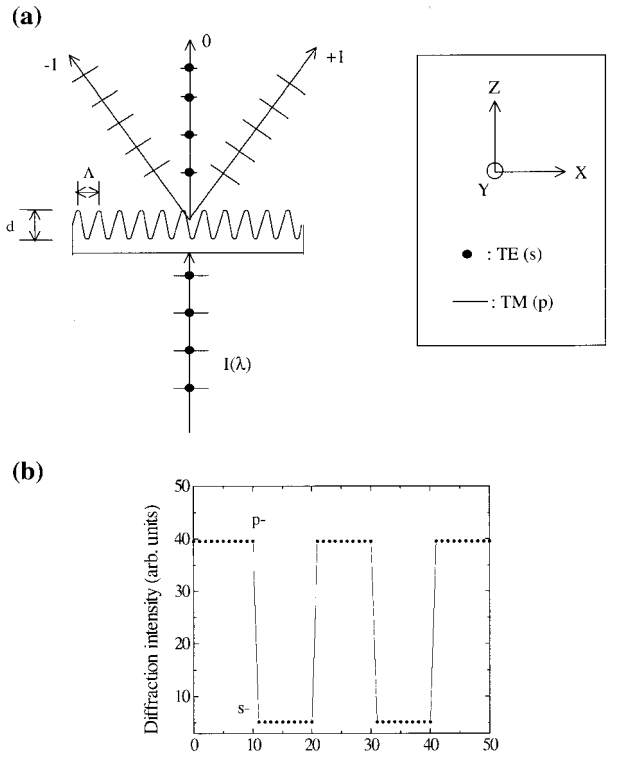

Fig. 17 (a) Schematic of the SRG used as polarization discriminator, (b) Polarization content of the +1 diffracted beam for an unpolarized probe beam at 633 nm.

3. Liquid crystal anchoring. Liquid crystal (LC) optical elements in various electro-optic devices require properly treated surfaces, which control alignment of the LC molecules.[99,100] The rubbing method is widely used in preparation of alignment layers in the industrial production of LC displays.[101] There has been an ongoing debate on the mechanism of LC alignment on the rubbed polymer surfaces. Two mechanisms have been proposed. One involves a long range interaction due to surface microgrooves generated by the rubbing process.[102] It was demonstrated that microgroove structures can induce alignment of LCs because elastic energy of LC molecules is minimized when the molecules lie along the grooves.[103–105] The second mechanism emphasizes the short-range interaction between LCs and the functional groups on the polymer surface, which become oriented during the rubbing process.[105,106] The relative importance between these two effects has not been clearly established, because the two effects co-exist and independent control of these two effects is not easily feasible.

Since both the microgroove structures and orientation of the functional groups could be produced and independently controlled in the azo polymer films, we investigated the relative importance of these two anchoring effects in the system by a simple separate control of the groove and the molecular orientation.

LC (nematic LC mixtures, E7 from Merck) cells were constructed using two polymer films containing surface gratings with different preferential orientation of azobenzene groups. After fabrication of two surface gratings with surface modulation of 120 nm with p-polarized beams, we re-exposed one of the gratings to a linearly polarized Ar^+ laser beam with the polarization direction parallel to the groove direction so that the orientation of azobenzene groups lies perpendicular to the groove direction. A AFM scan of re-exposure region showed about 100 nm surface modulation. This configuration is illustrated in Fig. 18.

The fabricated LC cell was observed between two polarizers. The area inside the exposed region clearly showed a twisted

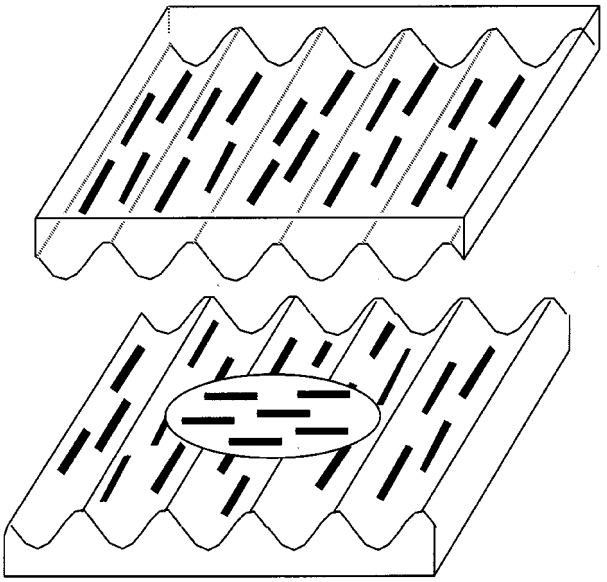

Fig. 18 Schematic for liquid crystal anchoring using SRG.

nematic structure. This indicates that the LCs adjacent to the re-exposed region were reoriented to the final direction of the azobenzene orientation leading to the twisted nematic configuration. Therefore, under the conditions we used, we have found that the anchoring effect of LCs due to the molecular interactions is stronger than that due to the surface topology.

In case of a LC cell sandwiched with the gratings recorded with a polarization direction 45° with respect to the s-polarization state, homogeneous alignment of LC molecules was not obtained. In this case no linear birefringence was observed throughout the exposed region because the polarization direction of the interference pattern varies periodically. Thus if we maintain the surface topology but remove the preferential orientation of azobenzene groups, no alignment occurs. The results confirmed that in this system molecular alignment of

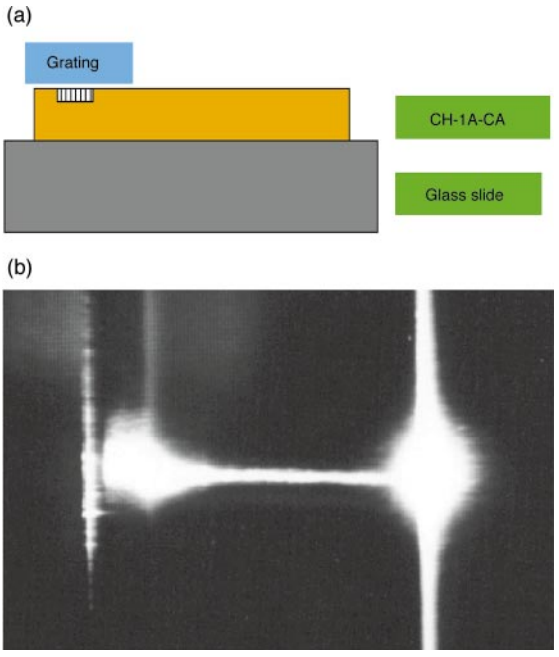

Fig. 19 (a) Schematic diagram of the slab waveguide of an azo polymer having a SRG written on it; (b) Photograph of the 830 nm laser light guided in the azopolymer waveguide. The laser light was coupled into the waveguide by the grating on the left and propagated to the right.

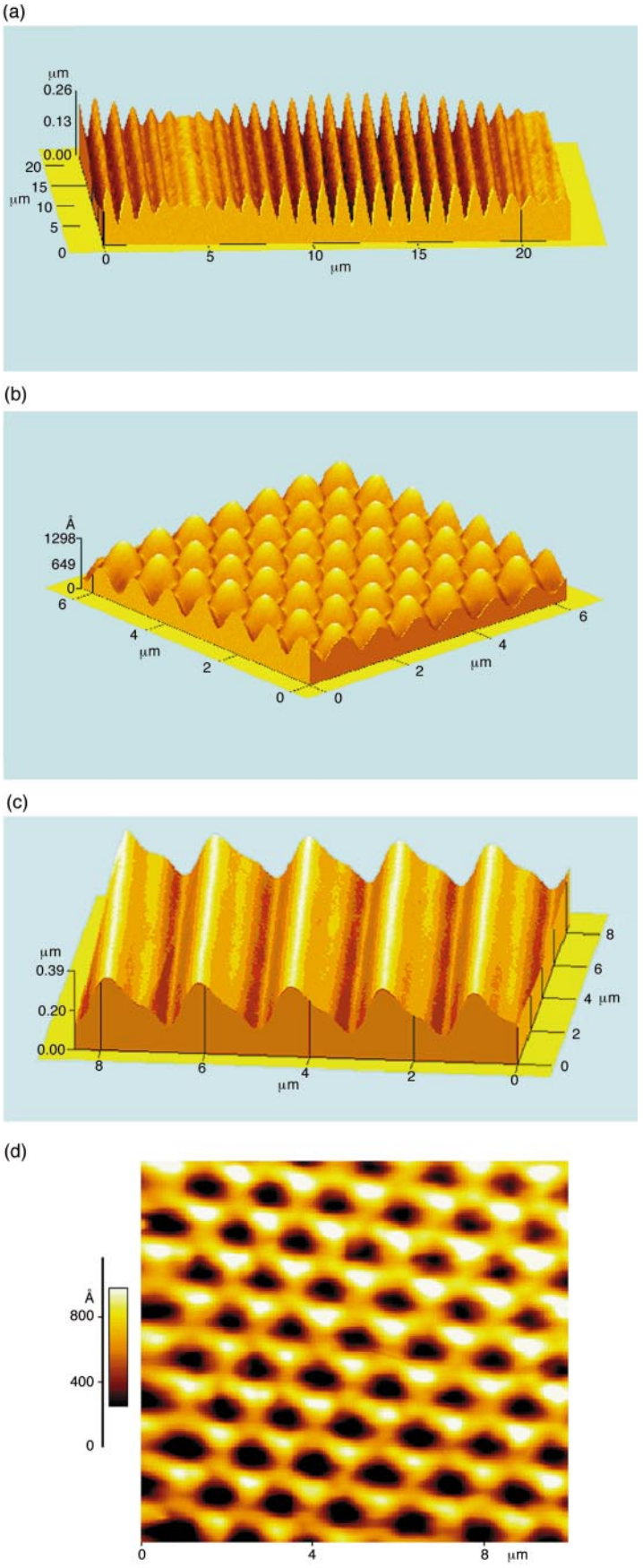

Fig. 20 Surface relief patterns formed on azo polymer films. (a) Beat structure; (b) Orthogonal gratings; (c) Fourier synthesized blazed grating; (d) Hexagonal pattern due to three beam interference.

azobenzene groups in anchoring the LCs plays the dominant role compared to surface topology effects.

4. Waveguide couplers. Diffraction gratings have been extensively used as input and output couplers and as feedback elements in integrated optics.[107] However, these gratings were traditionally made using multi-step photolithographic techniques.[108,109] The recently developed single step photofabrication process of SRG has offered for a quick formation of grating couplers with desired periods. Utilization of this one-step fabrication of surface gratings as slab waveguide couplers has been demonstrated. Fig. 19(a) shows a schematic diagram of a slab waveguide of an azo polymer (CH-1A-CA) with a surface relief grating written on it. The azo polymer film with a thickness of 1.31 μm was prepared by spin coating on a pre-cleaned glass slide substrate. The refractive index of the polymer was then measured to be 1.646 at 830 nm. The refractive index of the substrate at this wavelength is 1.510. The grating with a spacing of 485 nm and modulation amplitude of 250 nm was photofabricated at 488 nm. The sample was then positioned on a rotation stage. A diode laser at 830 nm was used as the light source. A photodetector in conjunction with a computer was utilized to monitor the coupling process. High coupling efficiency of about 20% has been obtained. A CCD camera was employed to capture the image when the laser light was coupled into the waveguide. Fig. 19(b) shows a photograph of the laser light guided in the waveguide. Paterson *et al*. recently demonstrated grating coupling and design of an optical filter based on a similar design.[107]

5. Intricate surface structures. Our understanding of the process and some of the advantageous features discussed in this article on the photofabrication of SRG on the azo functionalized polymer films are put to best use in intricately structuring the polymer surfaces. Fig. 20(a) is a well-defined beat structure recorded sequentially with two wavelengths, 488 and 514 nm at a fixed writing angle. The beat period is $\approx$19 μm. The resulting surface structure is close to the simple superposition of the two recording waves. When two gratings are recorded orthogonally to each other at the same place, the resulting '*egg-crate*' like structure is shown in Fig. 20(b). The gratings are highly symmetrical and identical and are indistinguishable. Fourier synthesized blazed grating is fabricated on the polymer film surface by superposing two gratings with different spacing (Fig. 20(c)). When three beams of appropriate polarization coherently interfere[110] on the azo polymer film surface, the resulting hexagonal '*honeycomb*' pattern formed is shown in Fig. 20(d). Thus by a simple superposition of various recording patterns, intricate surface structures can be fabricated on the azo functionalized polymer films. This opens an entirely new approach for fabricating diffractive optical elements.

Summary

Since the discovery of unusual light driven polymer mass transport on azo functionalized polymer solid films, a variety of applications have already been realized. Photofabrication of SRGs and other patterns in combination with the well-established photoanisotropic properties of azo polymers will certainly be utilized in other novel devices. In this article, we have reviewed this all-optical fabrication of SRGs in different classes of azo functionalized polymer films. Each of the different azo polymer system discussed has its own advantages. While a number of approaches to new material design and synthesis were presented, clearly opportunities abound and the optimal macromolecules for the specific application are continuing to be developed. Important new understanding about the nature of the surface deformation process and the relationship between the light pattern and the transport of the macromolecules is evolving. While the photonic nature of the deformation process is clearly realized, the photomechanical response of the polymer molecules and the film material itself is multifaceted and complex. This will be an important area for further investigation.

Acknowledgements

We gratefully acknowledge the financial support from the Office of Naval Research (ONR) and the National Science Foundation (NSF).

References

1 V. Weiss, A. A. Friesem and V. A. Krongauz, *Opt. Lett.*, 1993, **18**, 1809.
2 T. Huang and K. H. Wagner, *Appl. Opt.*, 1993, **32**, 1888.
3 V.P. Pham, T. Galstyan, A. Granger and R. A. Lessard, *Jpn. J. Appl. Phys.*, 1997, **36**, 429.
4 A. Yacoubian and T. M. Aye, *Appl. Opt.*, 1993, **32**, 3073.
5 T. Ikeda and O. Tsutsumi, *Science*, 1995, **268**, 1873.
6 J. M dos Santos and L. M. Bernardo, *Appl. Opt.*, 1997, **36**, 8935.
7 J. R. Wendt, G. A. Vawter, R. E. Smith and M. E. Warren, *J. Vac. Sci. Technol. B*, 1997, **15**, 2946.
8 E. Kim, G. M. Whitesides, L. K. Lee, S. P. Smith and M. Prentiss, *Adv. Magn. Reson.*, 1996, **8**, 139.
9 S. S. Lee, S. Garner, W. H. Steoer and S. Y. Shin, *Appl. Opt.*, 1999, **38**, 530.
10 M. Dumont, G. Froc and S. Hosotte, *Nonlinear Opt.*, 1995, **9**, 327.
11 J. Kato, I. Yamaguchi and H. Tanaka, *Opt. Lett.*, 1996, **21**, 767.
12 G. Sudesh Kumar and D. C. Neckers, *Chem. Rev.*, 1989, **89**, 1915.
13 H. Rau, 'Photoisomerization of azobenzenes,' in *Photochemistry and Photophysics*, ed. F. J. Rabeck, CRC, Boca Raton, FL, 1990, vol. 2, ch. 4, pp. 119–141.
14 S. Xie, A. Natansohn and P. Rochon, *Chem. Mater.*, 1993, **5**, 403.
15 *Photochromism*, *Molecules and Systems*, ed. H. Durr, Elsevier, New York, 1990.
16 T. Todorov, L. Nikolova, N. Tomova and V. Dragastinova, *Opt. Quantum Electron.*, 1981, **13**, 209.
17 T. Todorov, L. Nikolova, N. Tomova and V. Dragastinova, *IEEE J. Quantum Electron.*, 1986, **QE-22**, 1262.
18 T. Todorov, L. Nikolova and N. Tomova, *Appl. Opt.*, 1984, **23**, 4309.
19 T. Todorov, L. Nikolova and N. Tomova, *Appl. Opt.*, 1984, **23**, 4588.
20 L. Nikolova and T. Todorov, *Opt. Act.*, 1984, **5**, 579.
21 T. Todorov, L. Nikolova, K. Stoyanova and N. Tomova, *Appl. Opt.*, 1985, **24**, 785.
22 Sh. D. Kakichashivili and B. N. Kilosanidze, *Opt. Spectrosc.*, 1988, **65**, 243.
23 T. Huang and K. H. Wagner, *IEEE J. Quantum Electron.*, 1995, **31**, 372.
24 T. Huang and K. H. Wagner, *J. Opt. Soc. Am. B*, 1996, **13**, 282.
25 P. Rochon, E. Batalla and A. Natansohn, *Appl. Phys. Lett.*, 1995, **66**, 136.
26 D. Y. Kim, S. K. Tripathy, L. Li and J. Kumar, *Appl. Phys. Lett.*, 1995, **66**, 1166.
27 F. L. Labarthet, T. Buffeteau and C. Sourisseau, *J. Chem. Phys. B*, 1998, **102**, 2654.
28 P. Lefin, C. Fiorini and J. M. Nunzi, *Opt. Mater.*, 1998, **9**, 323.
29 M. Itoh, K. Harada, H. Matsuda, S. Ohnishi, A. Parfenov, N. Tamaoki and T. Yatagi, *J. Phys. D: Appl. Phys.*, 1998, **31**, 463.
30 L. Andruzzi, A. Altomare, F. Ciardelli, R. Solaro, S. Hvilsted and P. S. Ramanujam, *Macromolecules*, 1999, **32**, 448.
31 Z. Sekkat, J. Wood, E. F. Aust, W. Knoll, W. Volksen and R. D. Miller, *J. Opt. Soc. Am. B*, 1996, **13**, 1713.
32 J. Si, T. Mitsuyu, P. Ye, Z. Li, Y. Shen and K. Hirao, *Opt. Commun.*, 1998, **147**, 313.
33 T. D. Ebralidze and N. A. Ebralidze, *Appl. Opt.*, 1992, **31**, 4720.
34 T. D. Ebralidze, *Appl. Opt.*, 1995, **34**, 1357.
35 A. G. Chen and D. J. Brady, *Opt. Lett.*, 1991, **17**, 441.
36 S. Hvilsted, F. Andruzzi, C. Kulinna, H. W. Siesler and P. S. Ramanujam, *Macromolecules*, 1995, **28**, 2172.
37 N. C. R. Holme, P. S. Ramanujam and S. Hvilsted, *Appl. Opt.*, 1996, **35**, 4622.
38 L. M. Blinov, M. V. Kozlovsky, M. Ozaki, K. Skarp and K. Yoshino, *J. Appl. Phys.*, 1998, **84**, 3860.

39 T. Todorov, N. Tomova and L. Nikolova, *Opt. Commun.*, 1983, **47**, 123.
40 J. J. A. Couture and R. A. Lessard, *Appl. Opt.*, 1988, **27**, 3368.
41 Y. Shi, W. H. Steier, L. Yu, M. Chen and L. Dalton, *Appl. Phys. Lett.*, 1991, **59**, 2935.
42 P. Rochon, J. Gosselin, A. Natansohn and S. Xie, *Appl. Phys. Lett.*, 1992, **60**, 6.
43 C. Wang, H. Fei, Y. Yang, Z. Wei, Y. Qiu and Y. Chen, *Opt. Commun.*, 1999, **159**, 58.
44 Sh. D. Kakichashvili and T. N. Kvinikhidze, *Sov. J. Quantum Electron.*, 1975, **5**, 778.
45 Sh. D. Kakichashvili, *Sov. J. Quantum Electron.*, 1983, **13**, 1317.
46 W. J. Tomlinson, *Appl. Opt.*, 1975, **14**, 2456.
47 N. V. Kukhtarev, V. B. Markov, S. G. Odulov, M. S. Soskin and V. L. Vinetskii, *Ferroelectrics*, 1979, **22**, 949.
48 Z. Sekkat, J. Wood and W. Knoll, *J. Phys. Chem.*, 1995, **99**, 17226.
49 Z. Sekkat and M. Dumont, *Synth. Met.*, 1993, **54**, 373.
50 D. Y. Kim, L. Li, X. L. Jiang, V. Shivshankar, J. Kumar and S. K. Tripathy, *Macromolecules*, 1995, **28**, 8835.
51 X. L. Jiang, L. Li, J. Kumar, D. Y. Kim, V. Shivshankar and S. K. Tripathy, *Appl. Phys. Lett.*, 1995, **68**, 2618.
52 X. L. Jiang, L. Li, J. Kumar, D. Y. Kim and S. K. Tripathy, *Appl. Phys. Lett.*, 1998, **72**, 2502.
53 S. K. Tripathy, D. Y. Kim, T. S. Lee, X. L. Jiang, L. Li and J. Kumar, *Polym. Prepr.*, 1996, **37**, 123.
54 R. Birabassov, N. Landraud, T. V. Galstyan, A. Ritcey, C. G. Bazuin and T. Rahem, *Appl. Opt.*, 1998, **37**, 8264.
55 M. Ho, C. Barrett, J. Patersen, M. Esteghamatian, A. Natansohn and P. Rochon, *Macromolecules*, 1996, **29**, 4613.
56 B. Mandal, R. Jeng, J. Kumar and S. K. Tripathy, *Makromol. Chem., Rapid Commun.*, 1991, **12**, 607.
57 F. Dong, E. Kodoumas, S. Couris, Y. Shen, L. Qui and X. Fu, *J. Appl. Phys.*, 1997, **81**, 7073.
58 J. G. Victor and J. M. Tokelson, *Macromolecules*, 1987, **20**, 2241.
59 C. Barrett, A. Natansohn and P. Rochon, *J. Phys. Chem.*, 1996, **100**, 8836.
60 X. G. Wang, J. Chen, S. Marturunkakul, L. Li, J. Kumar and S. K. Tripathy, *Chem. Mater.*, 1997, **9**, 45.
61 X. G. Wang, L. Li, J. Chen, S. Marturunkakul, J. Kumar and S. K. Tripathy, *Macromolecules*, 1997, **30**, 219.
62 X. G. Wang, S. Balasubramanian, L. Li, X. L. Jiang, D. J. Sandman, M. F. Rubner, J. Kumar and S. K. Tripathy, *Macromol. Rapid Commun.*, 1997, **18**, 451.
63 N. K. Viswanathan, S. Balasubramanian, L. Li, J. Kumar and S. K. Tripathy, *J. Phys. Chem. B*, 1998, **102**, 6064.
64 F. L. Labarthet, T. Buffeteau and C. Sourisseau, *J. Phys. Chem. B*, 1998, **102**, 5754.
65 T. Fukuda, H. Matsuda, N. K. Viswanathan, S. K. Tripathy, J. Kumar, T. Shiraga, M. Kato and H. Nakanishi, *J. Synth. Met.*, 1999, in the press.
66 M. Amano and T. Kaino, *Chem. Phys. Lett.*, 1990, **170**, 352.
67 T. S. Lee, D. Y. Kim, X. L. Jiang, J. Kumar and S. K. Tripathy, *Mol. Cryst. Liq. Cryst.*, 1998, **95**, 316.
68 T. S. Lee, D. Y. Kim, X. L. Jiang, L. Li, J. Kumar and S. K. Tripathy, *J. Polym. Sci. A*, 1998, **36**, 283.
69 M. Sukwattanasinitt, X. Wang, L. Li, X. L. Jiang, J. Kumar, S. K. Tripathy and D. J. Sandman, *Chem. Mater.*, 1998, **10**, 27.
70 T. Masuda and M. Teraguchi, *Polym. Prepr.*, 1998, **39**, 283.
71 K. S. Alva, T. S. Lee, J. Kumar and S. K. Tripathy, *Chem. Mater.*, 1998, **10**, 1270 and references therein.
72 W. Liu, S. Bian, L. Li, J. Kumar, L. Samuelson and S. K. Tripathy, 'Enzymatic synthesis of photoactive poly(4-phenylazophenol)' submitted to *Chem. Mater.*, 1999.
73 S. K. Tripathy, D. Y. Kim, N. K. Viswanathan, S. Balasubramanian, W. Liu, P. Wu, S. Bian, L. Samuelson and J. Kumar, *J. Synth. Met.*, 1999, in the press.
74 M. Eich, J. H. Wendroff, B. Reck and H. Ringsdorf, *Makromol. Chem. Rapid. Commun.*, 1987, **8**, 59.
75 M. Eich and J. H. Wendroff, *Makromol. Chem. Rapid. Commun.*, 1987, **8**, 467.
76 S. Hvilsted, F. Andruzzi and P. S. Ramanujam, *Opt. Lett.*, 1992, **17**, 1234.
77 N. C. R. Holme, P. S. Ramanujam and S. Hvilsted, *Opt. Lett.*, 1996, **21**, 902.
78 M. Eich and J. Wendroff, *J. Opt. Soc. Am. B*, 1990, **7**, 1428.
79 L. Nikolova, T. Todorov, M. Ivanov, F. Andruzzi, S. Hvilsted and P. S. Ramanujam, *Appl. Opt.*, 1996, **35**, 3835.
80 P. S. Ramanujam, N. C. R. Holme and S. Hvilsted, *Appl. Phys. Lett.*, 1996, **68**, 1329.
81 N. C. R. Holme, L. Nikolova, P. S. Ramanujam and S. Hvilsted, *Appl. Phys. Lett.*, 1997, **70**, 1518.
82 I. Naydenova, L. Nikolova, T. Todorov, N. C. R. Holme, P. S. Ramanujam and S. Hvilsted, *J. Opt. Soc. Am. B*, 1998, **15**, 1257.
83 N. C. R. Holme, L. Nikolova, S. Hvilsted, P. H. Ramussen, R. H. Berg and P. S. Ramanujam, *Appl. Phys. Lett.*, 1999, **74**, 519.
84 T. G. Pedersen, P. M. Johansen, N. C. R. Holme, P. S. Ramanujam and S. Hvilsted, *Phys. Rev. Lett.*, 1998, **80**, 89.
85 N. K. Viswanathan, S. Balasubramanian, L. Li, J. Kumar and S. K. Tripathy, submitted to *Jpn. J. Appl. Phys.*, 1999.
86 S. Bian, L. Li, J. Kumar, D. Y. Kim, J. Williams and S. K. Tripathy, *Appl. Phys. Lett.*, 1998, **73**, 1817.
87 C. J. Barrett, P. Rochon and A. Natansohn, *J. Chem. Phys.*, 1998, **109**, 1505.
88 P. Lefin, C. Fiorini and J. M. Nunzi, *Pure Appl. Opt.*, 1998, **7**, 71.
89 G. Decher, *Science*, 1997, **277**, 1232.
90 J. Kumar, L. Li, X. L. Jiang, D. Y. Kim, T. S. Lee and S. K. Tripathy, *Appl. Phys. Lett.*, 1998, **72**, 2096.
91 P. W. Smith, A. Ashkin and W. J. Tomlinson, *Opt. Lett.*, 1981, **6**, 284.
92 K. O. Hill, B. Malo, F. Bilodeau, D. C. Johnson and J. Albert, *Appl. Phys. Lett.*, 1993, **62**, 1035.
93 B. Malo, D. C. Johnson, F. Bilodeau, J. Albert and K. O. Hill, *Opt. Lett.*, 1993, **18**, 1277.
94 J. Nishii, H. Yamanaka, H. Hosono and H. Kawazoe, *Opt. Lett.*, 1996, **21**, 1360.
95 K. Tsunetomo and T. Koyama, *Opt. Lett.*, 1997, **22**, 411.
96 L. Li, X. L. Jiang, D. Y. Kim, J. Kumar and S. K. Tripathy, *Org. Thin Films Photon. Appl. Tech. Dig.*, 1997, **14**, 214.
97 J. J. Butler, M. A. Rodriguez, M. S. Malcuit and T. W. Stone, *Opt. Commun.*, 1998, **155**, 23.
98 M. Schmitz, R. Brauer and O. Bryngdahl, *Opt. Lett.*, 1995, **20**, 1830.
99 M. Schadt, H. Seiberle and A. Schuster, *Nature*, 1996, **381**, 212.
100 V. K. Gupta and N. L. Abbott, *Science*, 1997, **276**, 1533.
101 J. Cognard, *J. Mol. Cryst. Liq. Cryst. Suppl. Ser.*, 1982, **1**, 1.
102 D. W. Berreman, *Phys. Rev. Lett.*, 1972, **28**, 1683.
103 U. Wolff, W. Grenbel and H. Kruger, *Mol. Cryst. Liq. Cryst.*, 1973, **23**, 187.
104 B. Cull, Y. Shi, S. Kumar and M. Schadt, *Phys. Rev. E*, 1996, **53**, 3777.
105 J. M. Geary, J. W. Goodby, A. R. Kmetz and J. S. Patel, *J. Appl. Phys.*, 1987, **62**, 4100.
106 H. Kikuchi, J. A. Logan and D. Y. Yoon, *Mater. Res. Soc. Symp. Proc.*, 1994, **345**, 247.
107 J. Paterson, A. Natansohn, P. Rochon, C. L. Callender and L. Robitaille, *Appl. Phys. Lett.*, 1996, **69**, 3318.
108 R. G. Hunsperger, *Integrated Optics: Theory and Technology*, Springer series in Optical Sciences vol. 33, Springer-Verlag, Berlin, 1985.
109 R. Arnost, *Photoreactive polymers: The Science and Technology of resists*, John Wiley, New York, 1989.
110 S. R. Cooper, D. W. Tomkins and M. Petty, *Opt. Lett.*, 1997, **22**, 357.

Paper 9/02424G